

defined and is responsible for Fe²⁺-binding, dimerization, and DNA binding. A partial X-ray crystallographic structure demonstrated that the C-terminal domain (80 aa residues) is structurally similar to eucaryotic SH3 domains, but the functional role of this domain in repressor activity was unknown. In this project, we used multidimensional heteronuclear NMR methods to obtain complete, sequential chemical shift assignments, and to determine a high-resolution structure of residues 130-226 of the intact repressor in solution (Figure 1). Residues preceding A147 were highly mobile in solution and adopted a random coil conformation. Residues A147-L226 form an independently-folding domain consisting of five β -strands and three helices arranged into a partially orthogonal, two-sheet β -barrel, similar to the structure observed in the crystalline Co²⁺-bound complex of full-length DtxR, and to that of eucaryotic SH3 domains.

SH3 domains are small proteins that mediate protein-protein interactions that occur to regulate protein activity and signal transduction in eucaryotic cells by binding to proline-rich regions of proteins. Proteins structurally homologous to SH3 domains had previously been identified from prokaryotic sources, but their functional roles were not identified. We used chemical shift perturbation studies to demonstrate that a proline-rich peptide corresponding to residues R125- G139 of intact DtxR binds to the C-terminal domain in a pocket formed by r residues in β -strands 2, 3, and 5, and in helix 3. Binding of the proline-rich peptide by the C-terminal domain of DtxR represents the first demonstration of a functional

SH3-like domain in a prokaryotic organism, and suggests that the C-terminal domain functions to regulate repressor activity. The strong sequence homology between DtxR and other members of this protein family, which includes virulence proteins from organisms causing tuberculosis, syphilis, and leprosi, suggests that our model, if valid, represents a general regulatory phenomenon. This model for regulation by the C-terminal domain of DtxR also suggests novel routes to the development of nonmetal-ion activators of repressor activity, which should decrease the virulence of these organisms.

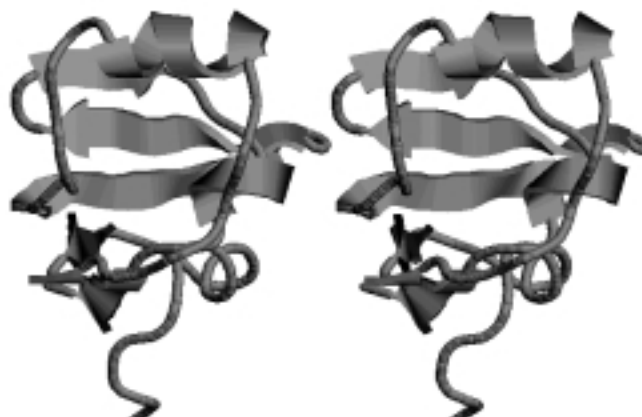


Figure 1. Structure of residues 130-226 of DtxR. A stereodigram is shown. To view the structure in stereo, slightly cross your eyes until the images line up and appear in 3D.

CHEMISTRY

Characterization of a Single Crystal Cubic Prussian Blue $\text{Co}_8(\text{tacn})_8(\text{CN})_{12}$ Cluster by Ion Trap and Fourier Transform Ion Cyclotron Resonance Mass Spectrometry with Microelectrospray Ionization

Andersen, U.N., Univ. of California at Berkeley, Chemistry
König, S., UC Berkeley, Chemistry
Leary, J.A., UC Berkeley, Chemistry
Freitas, M.A., NHMFL
Marshall, A.G., NHMFL/FSU, Chemistry

A single crystal of $\text{Co}_8(\text{tacn})_8(\text{CN})_{12}$ has been characterized by micro-electrospray mass spectrometry. Because a crystal is inherently purer than the solution in which the crystals form, the mass spectrum is inherently simpler and more readily resolved

and interpreted. The spectra obtained by use of FT-ICR, ion trap and quadrupole mass spectrometers show the +4, +3 and +2 charge states of the cluster. With the aid of a 9.4 T FT-ICR mass spectrometer it was possible to resolve the isotope pattern for each individual charge state. The data collected suggest that micro-electrospray renders spectra that are more specific to the intact molecule, whereas more fragmentation is induced under normal electrospray conditions. The present data suggest that micro-electrospray is a powerful tool for characterization of compounds that can be crystallized.

Acknowledgements: The authors acknowledge Prof. Jeffrey R. Long, Polly A. Berseth, and Julie L. Heinrich for synthesis of the compound presented herein. A. G. Marshall and M. A. Freitas also thank the NSF National High Field FT-ICR Mass Spectrometry Facility (CHE-94-13008), Florida State University, and the NHMFL at Tallahassee, Florida for their financial support.

¹ Andersen, U.N., *et al.*, *J. Am. Soc. Mass Spectrom.*, **10**, 352-354 (1999).

Synthesis of Structurally Diverse C-Linked AFGP Mimics

Ben, R.N., State Univ. of New York at Binghamton,
Chemistry

Eniade, A., SUNY-Binghamton, Chemistry

Hauer, L., SUNY-Binghamton, Chemistry

Antifreeze Glycoproteins (AFGPs) have the ability to inhibit the growth of ice crystals *in vivo*. These compounds are essential to the survival of organisms that inhabit subzero environments such as Arctic and Antarctic teleost fish. The structure of a typical AFGP is shown in Figure 1.

Since the ability to inhibit the growth of ice crystals is very attractive from a practical perspective, it is not surprising that these compounds have potential medical, industrial, and commercial applications. An attractive alternative to the isolation and purification of native AFGP is the rational design and synthesis of novel synthetic antifreezes with enhanced stability and activity. It is likely that the design of such compounds will be based closely on the structure of native AFGPs. Unfortunately, the mechanism by which AFGPs inhibit ice crystal growth is not well understood and this has prevented the rational design of such compounds.

In an effort to further elucidate the mechanism by which these glycoproteins function, our laboratory is conducting detailed structure-function studies using various synthetic AFGP mimics. Our synthetic strategy is centered on the preparation of structurally diverse building blocks that are assembled into C-linked AFGP mimics using conventional solid phase synthesis.

During a one-week period at the NHMFL in January, 1999, we performed a series of experiments using the 720 MHz NMR spectrometer on "first generation" building blocks that were previously prepared in our laboratory. Structures of these compounds are shown in Figure 2.

Routine one- and two-dimensional proton and heteronuclear experiments were performed on these building blocks with the purpose of confirming structure. Given that the Chemistry Department at SUNY-Binghamton possesses an aging 360 MHz NMR, the facilities at NHMFL are ideally suited for working with the complex glycoconjugates prepared in our laboratory. During the one-week period, a total of 30 experiments were performed on these building blocks. Assignment of proton and carbon resonances were made and the structure of each building block was confirmed independently. Additional two-dimensional experiments were performed to gain insight into the conformation of the saccharide moiety (relative to the backbone) in the divalent oligosaccharides derivatives.

Since January 1999, complex glycoconjugates have been prepared ranging from 1.5 to 5 Kdaltons using these building

blocks. Future trips to the NHMFL will utilize the NMR facilities to gain insight into the tertiary structure and solvation of these glycopolymers. Such studies are necessary to rationalize biological results.

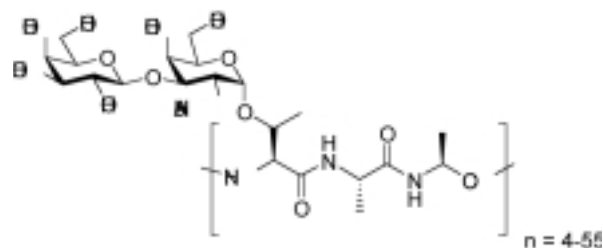


Figure 1. Typical antifreeze glycoprotein.

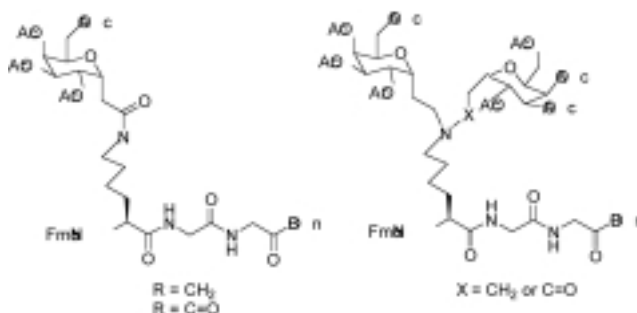


Figure 2. Building blocks of AFGP mimetics.

High Resolution ^{17}O NMR Study of Zeolites

Bull, L.M., Institut des Materiaux Jean Rouxel, Nantes,
France

Samoson, A., National Institute of Chemical Physics and
Biophysics, Tallinn, Estonia

Zeolites are currently used in many important industrial processes, including catalysis, separation, and ion-exchange reactions. Understanding where the active sites are in these materials and the relationship between the structure and their properties is essential if the goal of tailoring the structure of a material in order for it to exhibit a particular property is to be achieved. High resolution solid-state ^{17}O NMR is a characterization technique that can potentially be used to directly view active sites in zeolitic materials as it is a tool that is sensitive to the local environment around the oxygen, and the oxygen is the element that is intimately involved in the reactions listed above. Due to the magnitude of the quadrupole interaction in these materials (4-6 MHz), however, only poorly resolved spectra can be observed at low magnetic field strengths. We have now demonstrated using a variety of spectrometers operating at different field strengths, including the 500, 600, and 720 MHz spectrometers at Tallahassee, that it is possible to fully resolve each oxygen site in a zeolite. The importance of using different field strengths is illustrated in the figure. As the field strength increases the competition between the two mechanisms responsible for the separation and width of

the peaks (the chemical shift and the quadrupolar interaction) favors higher resolution spectra, and thus the ability to observe each individual oxygen site. The missing link between the NMR results and the structure of the zeolite is then completed by using quantum mechanical calculations of the experimentally determined NMR parameters in collaboration with Professor Joachim Sauer at the Humboldt University in Berlin. Although this work is only in its early stages, we believe that this use of solid-state NMR can be extended to study oxides in general, which constitute the majority of industrially applied materials today.

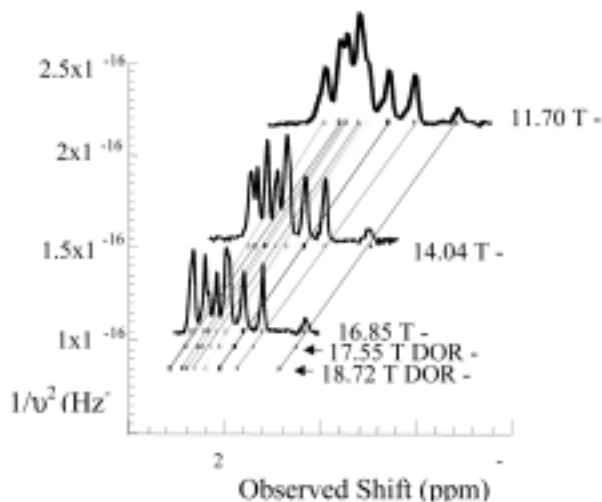


Figure 1. ^{17}O DOR NMR spectra of zeolite Siliceous Ferrierite as a function of resonance frequency.

Conformations of Peptide Fragments from FKBP: Comparison with the Native and Urea-Unfolded States

Callihan, D.E., FSU, Chemistry

Logan, T.M., NHMFL/FSU, Chemistry

Structural characterization of the denaturant-unfolded states of proteins is important to understand the protein folding process. Here, a combination of CD and NMR spectroscopies was used to investigate the importance of local versus non-local interactions in generating non-random structure in the urea-unfolded state of the FK506 binding protein (FKBP) by determining the helix-forming tendency of seven peptide fragments corresponding to the entire sequence of FKBP in aqueous buffer and in trifluoroethanol solutions. Fragments were chosen to overlap with regions of non-random conformational averaging in unfolded FKBP. We reasoned that if the peptide fragments were (at least) as ordered the same residues in unfolded FKBP, then local amino acid interactions dictate the conformational averaging in unfolded FKBP.

As expected, the helix forming tendencies varied with amino acid sequence, with fragments corresponding to the α -helix and β -strands 2 and 3 exhibiting the highest helix propensity.

These regions generally showed measurable non-random conformational averaging in unfolded FKBP. In contrast, the fragment corresponding to β -strand I and a long, disordered loop showed essentially no tendency to form helix, even in concentrated TFE solutions. These residues were essentially random coil in unfolded FKBP. Therefore, the helix-forming tendency in TFE appears to be a reasonable indicator of structure formation in an unfolded protein. 2D NMR was used to further characterize each of these peptide fragments to provide a means to compare them to the conformational averaging in unfolded FKBP. Surprisingly, each fragment appeared more random in aqueous solution (strongly folding conditions) than in FKBP in concentrated urea (strongly unfolding conditions) based on analysis of 2D homonuclear NOESY spectra collected under a variety of conditions. The NOE interaction is strongly dependent on molecular rotational correlation times, and can be near zero for peptides of this size. The following studies support our conclusion, however, that the peptides were more disordered than unfolded FKBP. First, all NOE intensities for these peptides were negative, as were NOE intensities for unfolded FKBP. Second, there were no differences in NOE spectra collected at 11.7 or 16.8 T. Third, NOE patterns were identical in NOESY or ROESY spectra, and fourth, addition of 5 or 10% glycerol had no effect on the observed NOE patterns.

Based on these results, we conclude that conformational averaging in urea-unfolded FKBP reflects the conformational preferences of the local amino acid sequence, but these local interactions are not sufficient to induce non-random conformational averaging in unfolded FKBP. We propose that non-specific, long-range hydrophobic interactions, present in a long polymer, but absent in short polymers, serve to promote structure in regions of unfolded proteins that have a high inherent helicity. This model supports the nucleation-condensation model for folding, but extends the concept of long-range interactions to occurring prior to the transition state.

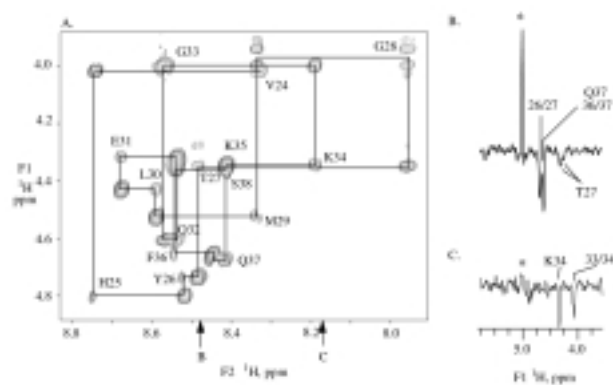


Figure 1. Expansion of a 250 ms NOESY spectrum of a peptide fragment collected in aqueous phosphate buffer. Assignments are indicated in the figure. One dimensional traces were taken from a 2D ROESY spectrum at the positions corresponding to the arrows. These spectra clearly show an absence of medium range NOE interactions in the short peptides.

Structural Characterization of Long Fragments of the FK505 Binding Protein as Models of Early Events in Protein Folding

Callihan, D.E., FSU, Chemistry

King, T.D., FSU, Chemistry

Logan, T.M., NHMFL/FSU, Chemistry

All current models of protein folding process agree that the earliest events in protein folding include collapse to a compact denatured state, driven by the hydrophobic effect, and formation of secondary structure, driven primarily by local amino acid conformational preferences. The temporal order and extent of interaction between these two processes, however, is of great debate. Previously, we showed that conformational averaging in unfolded proteins appears to depend on a weak hydrophobic "center" present in denaturant-unfolded proteins. In this project, we are using multidimensional NMR spectroscopy to characterize the conformational averaging in long fragments of the FK506 binding protein (FKBP). By increasing the length of these peptides, we hope to answer the question of how long a peptide needs to be to resemble a denatured protein, and to identify the residues responsible forming the hydrophobic center of unfolded FKBP.

The first step in this project required the generation of a convenient system for producing isotope-labeled protein fragments. Toward this end, we constructed a fusion between FKBP and the maltose binding protein. Protein fragments were generated using the polymerase chain reaction, expressed in bacteria, purified, cleaved, and purified away from the MBP carrier protein. Several fragments have been generated and two have been structurally characterized, corresponding to approximately 50% and 75% of the total length of FKBP. The chemical shifts for these fragments were assigned using standard triple resonance experiments, and structural information collected based on chemical shifts, scalar coupling constants, and dipolar cross-correlation effects (NOEs). The NMR data show that the amount of structure in each peptide increases with decreasing denaturant concentration, emphasizing the importance of hydrophobic contacts in structure formation. Similarly, the amount of structure increases with increasing fragment length. These studies support the nucleation-condensation model of folding, which suggests that folding proceeds with a combination of long-range hydrophobic interactions that stabilize local conformational preferences.

Acknowledgements: This work was supported by NIH and NSF.

Gas Phase Activation Energy for Unimolecular Dissociation of Biomolecular Ions Determined by Focused Radiation for Gaseous Multiphoton Energy Transfer (FRAGMENT)

Freitas, M.A., NHMFL

Hendrickson, C.L., NHMFL

Marshall, A.G., NHMFL/FSU, Chemistry

We present a novel approach for the determination of activation energy for the unimolecular dissociation of a large (>50 atoms) ion, based on measurement of unimolecular dissociation rate constant as a function of continuous-wave CO₂ laser power. Following a short (~1 s) induction period, CO₂ laser irradiation produces an essentially blackbody internal energy distribution, whose "temperature" varies inversely with laser intensity. The only currently available method for measuring such activation energies is Blackbody Induced Radiative Dissociation (BIRD). Compared to BIRD, FRAGMENT: (a) eliminates the need to

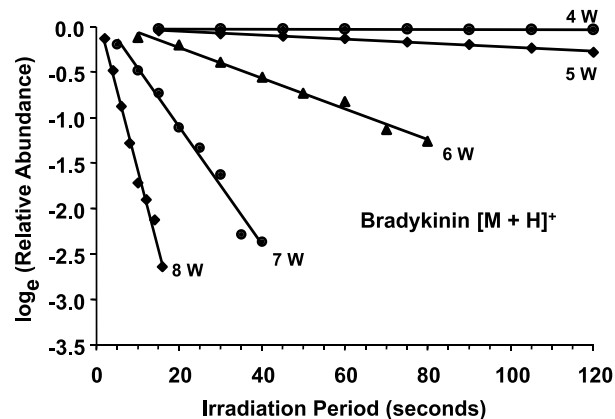


Figure 1. FRAGMENT Dissociation of bradykinin at various laser intensity and time.

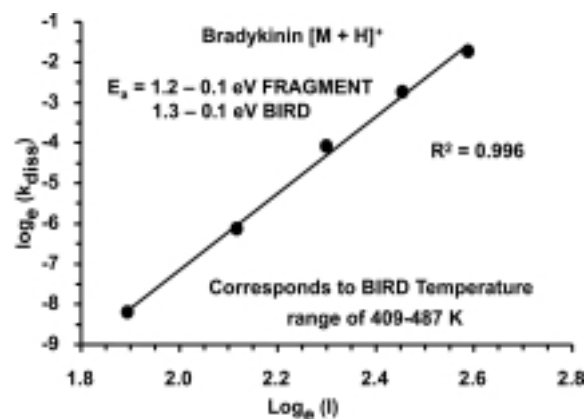


Figure 2. Correlation of FRAGMENT data with BIRD data for protonated bradykinin.

heat the surrounding ion trap and vacuum chamber to each of several temperatures (each requiring hours for temperature equilibration); (b) offers a three-fold wider range of effective blackbody temperature; and (c) extends the range of applications to include initially cold ions (e.g., gas-phase H/D exchange). Our FRAGMENT-determined activation energy for dissociation of protonated bradykinin, 1.2 +/- 0.1 eV, agrees within experimental error to the value, 1.3 +/- 0.1 eV, previously reported by Evan Williams et al. from BIRD experiments.

Acknowledgements: We thank John P. Quinn, Dan McIntosh (National High Magnetic Field Laboratory) for their technical expertise and helpful discussion. This work was supported by NSF (CHE-93-22824), the NSF National High Field FT-ICR Facility (CHE-94-13008), Florida State University and the National High Magnetic Field Laboratory in Tallahassee, FL.

¹ Freitas, M.A., *et al.*, Rapid Commun. Mass Spectrom., **13**, 1639-1642 (1999).

Determination of Total Body Water in Humans by Deuterium NMR Spectroscopy

Kehayias, J.J., Tufts Univ., USDA Human Nutrition Research Center on Aging

Murali, N., NHMFL

Dupont, J., FSU, Nutrition, Food and Movement Sciences

Nutritional status is directly related to the amount and quality of fat free mass. Successful nutritional support of the diseased or the elderly results in the maintenance or increase of lean body mass. Total body water (TBW) is a simple index of lean tissue as it occupies 73% of its mass. Measuring total body water on the field can become an important tool for assessing nutritional status, testing the efficacy of pharmaceutical intervention and managing obesity. When combined with other measurements, water and its compartments provide a detailed description of body composition of the patient. All direct methods for measuring water in vivo are based on isotope dilution techniques. A known amount of water—labeled with O-18 or tritium or deuterium—is administered orally or intravenously. Three to five hours later a small (1-5 cc) blood or urine sample is collected and analyzed for its isotopic enrichment. From this measurement, TBW, the diluting volume, is calculated. The technique has been proven very successful because of the body's ability to reach equilibrium rapidly and completely even in disease. The clinical usefulness of the technique is limited by the time required for analyzing blood or urine samples in specialized laboratories (usually by ratio mass spectrometry).

The purpose of this project is to evaluate the capability of deuterium NMR analysis of blood serum and define the parameters of a dedicated portable NMR deuterium analyzer for field use.

The 720 MHz NMR spectrometer was used to observe deuterium nucleus (110.6 MHz). Liquid samples (600 µl each) were measured at room temperature. Deuterated butanol (tetra-butanol-d9) was used in the samples as internal standard. The reproducibility (one CV) of the area under the deuterium peak was better than 0.13% for high concentration samples (>0.1%). The reproducibility for the internal standard, however, was found to be 4.1% between samples. Similarly, low concentration D2O solutions had reproducibility of about 5%, most of which was attributed to the technique used for the area integration.

High field NMR spectroscopy has the sensitivity to measure natural concentrations of D2O in water, blood, and urine, and the chemical-shift resolution required for the use of deuterated butanol as internal standard. We found, however, that the precision of the instrument is only marginal when used with the manufacturer-supplied peak integration software, especially at the pre-dose low D2O concentrations. The advantage of internal-standard-NMR is the elimination of sample preparation. In future experiments we expect to focus on data analysis methods tailored to improving signal strength precision. The accuracy of the technique will be tested against ratio mass spectrometry.

Proton MAS NMR Studies of Human Bone and Bone Components

Kolodziejcki, W., Medical Univ. of Warsaw, Pharmacy
Kaflik-Hachulska, A., Medical Univ. of Warsaw, Pharmacy

Samoson, A., National Institute of Chemical Physics and Biophysics, Tallinn, Estonia

A human bone consists of organic fraction, which is mostly collagen, and inorganic fraction. It is widely accepted that the main component of the inorganic fraction of the bone is hydroxyapatite.

We performed comparative proton MAS NMR measurements of bone mineral and apatites of close chemical composition. Measurements were carried out at 832 MHz proton frequency, available with 32 mm bore superconducting magnet. The sample spinning frequency was 30-40 kHz.

The main features of hydroxyapatite spectrum are a peak at 5 ppm, mainly from residual water and from hydrogen bonded hydroxylic groups, and a peak at 0 ppm, assigned to structural hydroxyl groups not involved in hydrogen bonds.

The spectrum of human tabecular bone features relatively narrow collagen peaks in the background of signal from the mineral fraction. It is quite evident that resonance line of structural hydroxyl groups (0 ppm) is either missing or very weak. This signal is also missing in the spectrum of carbonatoapatite. The structure of carbonatoapatite is actually characterized by closest chemical composition with bone mineral, containing 5-10 wt% carbonate anions. A possible

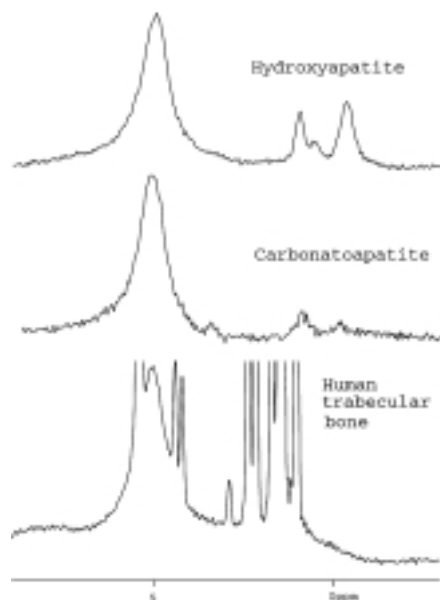


Figure 1. ^1H MAS (30–40 kHz) spectra at 832 MHz.

conclusion is that structural hydroxylic groups typical for hydroxyapatite are missing from the bone apatite, probably because of the presence of carbonate groups in this material. This is in accordance with former IR studies of animal bone¹ and proposed mineral composition of bone tissue².

¹ Rey, C., *et al.*, *J. Bone*, **16**, 583–586, (1995).

² Legros, R., *et al.*, *J. Chem. Res. (S)*, **8**, (1986) and references therein.

330 to 670 GHz EPR Studies of Canthaxanthin Radical Cation Stabilized on a Silica-Alumina Surface

Konovalova, T.A., Univ. of Alabama, Chemistry
 Krzystek, J., NHMFL
 Bratt, P.J., UF, Chemistry
 Van Tol, J., NHMFL
 Brunel, L.-C., NHMFL
 Kispert, L.D., Univ. of Alabama, Chemistry

We report the first example of a well-resolved 330–670 GHz EPR spectra of a carotenoid radical cation. At 9–250 GHz the carotenoid radical cation cannot be distinguished from other C-H π -radicals observed in powder and frozen glasses, since its g tensor cannot be resolved at these frequencies. The 330 GHz and higher frequency EPR spectra were resolved into two principal components of the g tensor. Spectral simulation indicated this to be the result of g -anisotropy where $g_{\parallel} = 2.0032$ and $g_{\perp} = 2.0023$. This type of g tensor is consistent with the theory for polyacene π -radical cations, which states that the g tensor becomes cylindrically symmetric with increasing chain length.¹ This also demonstrates that the symmetrical unresolved EPR line at 9 GHz is due to a carotenoid π -radical cation with electron density distributed throughout the whole chain

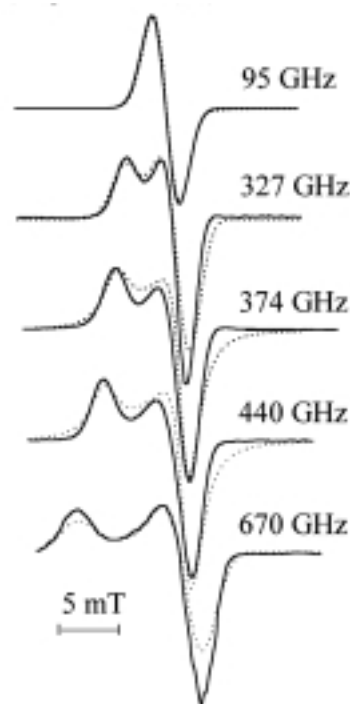


Figure 1. HF-EPR spectra of canthaxanthin radical cation: (solid) experimental, (dot) simulated.

as predicted by RHF-INDO/SP molecular orbital calculations. The lack of temperature dependence of the EPR linewidths over the range of 5 to 80 K suggests rapid rotation of methyl groups even at 5 K that averages out the proton couplings from three oriented β -protons.

The present work shows that the 330 to 670 GHz EPR measurements are sufficient to resolve the individual g tensor components and distinguish carotenoid radical cations from other C-H containing radicals, which have different symmetry.

¹ Stone, A.J., *Mol. Phys.*, **7**, 309 (1964).

Elucidation of the Electronic Structure of Manganese(III) Corrole Complexes

Krzystek, J., NHMFL
 Telser, J., Roosevelt Univ., Chemistry
 Hoffman, B.M., Northwestern Univ., Chemistry
 Licoccia, S., Univ. of Rome Tor Vergata, Italy, Chemistry,
 Science & Technology

Among cyclic tetrapyrroles, corroles have a structure that has been considered to be intermediate between that of a porphyrin and a corrin, having a direct link between the two pyrrole rings. Corroles have revealed some very interesting properties such as the capability of maintaining a planar conformation even when completely substituted at the peripheral positions.¹ Having three amino-like nitrogen atoms, a corrole behaves as a trianionic ligand and it may either stabilize high oxidation states for coordinated transition metal ions, or be easily oxidized to a

cation radical itself, the latter being the most common situation in solution.²

While transition metal porphyrins have been extensively studied, and their EPR and NMR spectra investigated in great detail for many years,³ much fewer studies on the corresponding metal corroles have been reported. Because of the similar ring structure of these two macrocycles, as well as the similarity of the corrole ring to the biologically relevant corrins, it is important to further characterize the metal complexes of corroles by magnetic resonance techniques.

Previous studies have shown that manganese corrolates exist in the solid state as square planar Mn(III) derivatives which exhibit an unusual coordination number of four.⁴ X-band EPR has been reported as silent for these complexes. We have therefore employed HF EPR, which has already proved effective in elucidating electronic structure of several Mn(III) complexes.^{5,6} The application of this technique to manganese corrolates will help defining its electronic structure and lead to a better understanding of the metal/ligand bonding in tetrapyrrolic complexes.

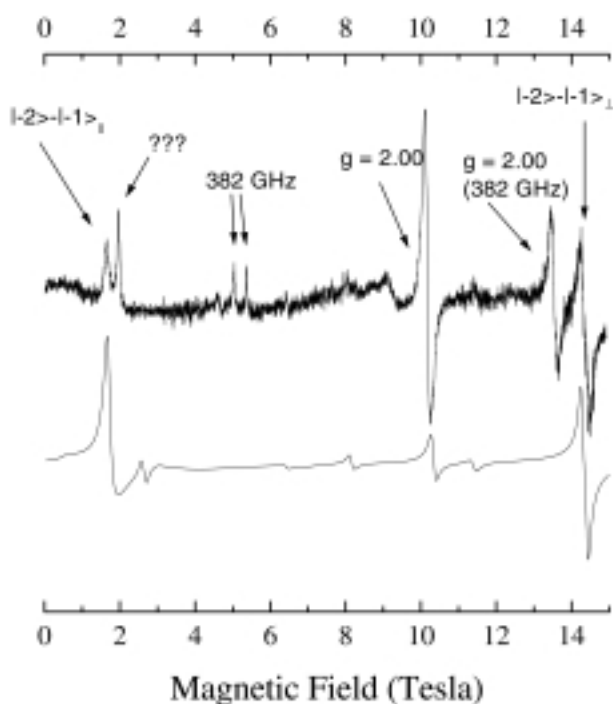


Figure 1. A 284 GHz experimental (top) and simulated (bottom) HF EPR spectrum of a (8,12-diethyl-2,3,7,13,17,18-hexamethylcorrolato) Manganese (III) KBr pellet at 4.5 K. Particular spin transitions are identified and labelled accordingly.

A sample HF EPR spectrum of polycrystalline (8,12-diethyl-2,3,7,13,17,18-hexamethylcorrolato) Manganese (III) is shown in Figure 1. This, and similar spectra allowed to calculate the spin Hamiltonian parameters characterizing the d^4 , $S = 2$ spin state of Mn(III) which are: $D = -2.630 \text{ cm}^{-1}$, $E = +0.015 \text{ cm}^{-1}$, $g_x = g_y = 2.02$, $g_z = 2.00$. It is remarkable for the asymmetrical complex that its zfs tensor is almost axial; however, a small amount of rhombicity shows up in the parameter E, and results in a slight doubling of the perpendicular $|-2\rangle - |-1\rangle$ transition. The electronic structure determination of the complex under study is currently in progress but the spin Hamiltonian parameters already point to a similarity with (tetraphenylporphyrinato) Manganese (III) chloride, studied previously.⁶

¹ Licoccia, S., *et al.*, Structure and Bonding, **84**, 73 (1995).

² Cai, S., *et al.*, Inorg. Chem., in press.

³ Walker, F.A., *et al.*, Biological Magnetic Resonance, Vol. 12: Molecules, L. J. Berliner, ed., Plenum Press, N.Y., 1993, pp. 133-274.

⁴ Licoccia, S., *et al.*, Inorg. Chem., **36**, 1564 (1997).

⁵ Goldberg, D.P., *et al.*, J. Am. Chem. Soc., **119**, 8722 (1997).

⁶ Krzystek, J., *et al.*, Inorg. Chem., **38**, 6121 (1999).

High Frequency and High Field EPR Spectroscopy of Manganese(III) Porphyrins and Me₂dbm Complexes: Influence of Axial Ligand on Electronic Structure

Krzystek, J., NHMFL

Telser, J., Roosevelt Univ., Chemistry

Knapp, M.J., Univ. of California at Berkeley, Biochemistry

Hendrickson, D.N., Univ. of California at San Diego, Chemistry

Brunel, L.-C., NHMFL

A very large number of metalloporphyrins are known to be of great importance in several biological and chemical systems. For example, metalloporphyrins are found as cofactors in many proteins, such as in the cytochromes.¹ Metalloporphyrins are also relevant as oxidation catalysts, and as building blocks for molecular magnets, as are Me₂dbm complexes. In many cases, the metal ion complexed by the porphyrin or Me₂dbm is paramagnetic and can be investigated by EPR (e.g., Fe³⁺ and Mn²⁺).¹ When the paramagnetic ion is integer spin (e.g., Fe²⁺ and Mn³⁺), however, the geometry imposed by the ligand often leads to large zero-field splittings that preclude observation of EPR spectra using conventional spectrometers. High frequency, high field EPR (HF EPR), in contrast, employs microwave quanta and magnetic fields sufficiently large ($\nu > 90 \text{ GHz}$; B up to 25 T) so that EPR spectra are indeed observable.

We have begun a broad project to apply HF EPR to investigate the electronic structure of porphyrinic complexes of integer spin transition metal ions, beginning with Mn³⁺ ($3d^4$, $S = 2$). We have previously studied Mn³⁺ complexed by TPP (tetraphenylporphyrin)^{2,3} and by Pc (phthalocyanin),³ in both

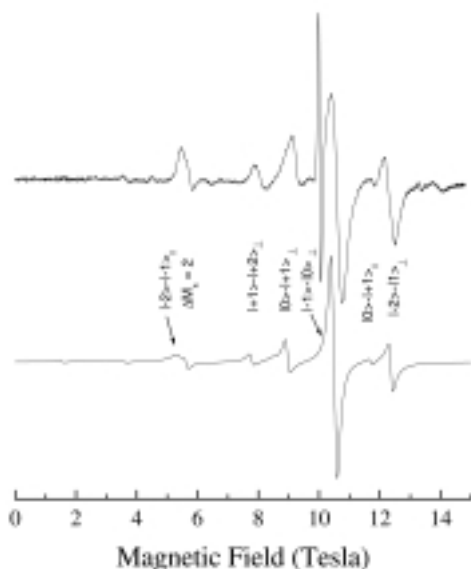


Figure 1. HF EPR spectrum of $\text{Mn}(\text{Me}_2\text{dbm})_2\text{Br}$ at 279 GHz and 15 K in eicosane mull: experimental spectrum (top) and spectrum simulated using $D = -1.46 \text{ cm}^{-1}$, $E = 0$, $g_{x,y} = 2.00$, $g_z = 1.97$ (bottom). Individual allowed and partially allowed transitions are identified. The sharp peak at 10 T is due to a Mn^{2+} impurity and is not reproduced in the simulation.

cases with an axial Cl^- ligand. We found that variation in the macrocyclic ligand causes relatively little change in electronic structure of Mn^{3+} . The current project extends this work to a series of complexes in which the axial ligand is systematically varied. The porphyrin ligand employed is OEP (2,3,7,8,12,13,17,18-octaethylporphyrin) and the axial ligands are Cl^- , Br^- , and I^- . We have also studied $\text{Mn}(\text{III})$ complexed with Me_2dbm where Hdbm is 1,3-diphenyl-1,3-propanedione, with Cl^- and Br^- as axial ligands.

All the $\text{Mn}(\text{OEP})\text{X}$ ($\text{X} = \text{Cl}^-$, Br^- , I^-) and $\text{Mn}(\text{Me}_2\text{dbm})_2\text{X}$ ($\text{X} = \text{Cl}^-$, Br^-) complexes show rich spectra, arising from the many transitions possible for axial $S = 2$ systems. The HF EPR spectra have been recorded at multiple microwave frequencies and at varying temperatures to provide a complete spectroscopic picture. They were subsequently analyzed using powder pattern simulation methods to provide spin Hamiltonian parameters approximately: $D = -2.2$ – -2.4 cm^{-1} , -1.1 – -1.5 cm^{-1} , -0.07 cm^{-1} , for $\text{X} = \text{Cl}^-$, Br^- , I^- , respectively. In all cases, $E = 0$, and $g = 2.00$, meaning that the systems are rigorously axial, as expected from the geometry of OEP and Me_2dbm . The results for $\text{Mn}(\text{OEP})\text{Cl}$ and $\text{Mn}(\text{Me}_2\text{dbm})_2\text{Cl}$ are in agreement with those found previously for $\text{Mn}(\text{TPP})\text{Cl}$ and $\text{Mn}(\text{Pc})\text{Cl}$,³ as expected since the ligand has a relatively small effect on electronic parameters. The effect of axial ligand is, in contrast, quite pronounced. The relatively weak-field iodo ligand leads to a nearly cubic symmetry, while bromo is an intermediate case. The results are discussed in terms of the overall electronic structure of $\text{Mn}(\text{OEP})\text{X}$ and $\text{Mn}(\text{Me}_2\text{dbm})\text{X}$ and in context of magnetic susceptibility studies on related complexes.⁴

¹ Palmer, G., *The Porphyrins*; vol. IV; New York: Academic Press, 1979; pp. 313-353.

² Goldberg, D.P., *et al.*, *J. Am. Chem. Soc.*, **119**, 8722 (1997).

³ Krzystek, J., *et al.*, *Inorg. Chem.*, **38**, 6121(1999).

⁴ Dugad, L.B., *et al.*, *Chem. Phys. Letters*, **104**, 353 (1984).

Application of a High-Resolution Superconducting NMR Probe in Natural Product Structure Determination

Logan, T.M., NHMFL/FSU, Chemistry

Murali, N., NHMFL

Wang, G.S., FSU, Institute of Molecular Biophysics

Jolivet, C., FSU, Chemistry

The signal strength in NMR depends on several factors, including sample-related factors such as concentration or number density, Boltzmann factor (or spin polarization), and instrument-related factors such as probe design, Q, noise-factor, and coil temperature. Sensitivity increases are typically pursued by optimizing coil geometry, sample concentration, and the external magnetic field. Operating the radiofrequency coils at cryogenic temperatures has been shown to significantly improve signal to noise ratios (SNR) in imaging with surface coils constructed of high temperature superconducting (HTS) ceramics. High-resolution NMR probes made of similar materials have been demonstrated, but their utility in practical applications has not been widely investigated. Here, we demonstrate significant increases in SNR obtained from a high-resolution NMR probe operating at 25 K that uses HTS ceramics for the r.f. transmit/receive circuitry. The advantages of this probe for natural product structure determination are demonstrated.

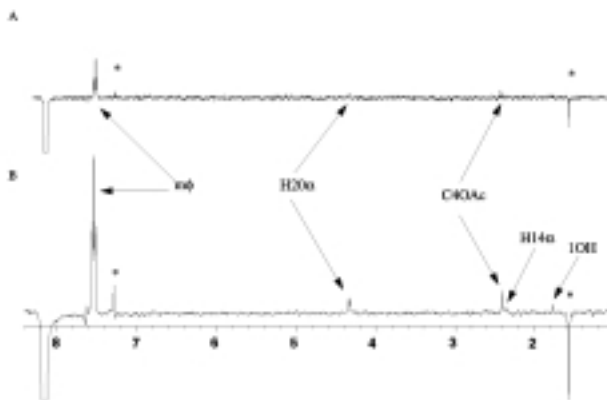


Figure 1. Comparison of NOE difference spectra collected on (A) the HTS probe and (B) a conventional probe.

The probe, operating at a ^1H frequency of 400 MHz, provides a SNR of 1691:1 on a 0.1% ethylbenzene sample, represents a substantial SNR improvement over the ca 450:1 obtained on the same instrument using a conventional triple-resonance probe. The lineshape of the probe was determined to be 7.3 / 14.1, somewhat higher than obtained using conventional probes. The probe gave a $16 \mu\text{s}$ 90° pulse measured with 9 dB attenuation of the 50W power on a CHCl_3 sample in acetone- d_6 . The r.f. homogeneity was 65%, measured as the ratio of the 450 / 90 pulse widths. r.f. linearity was poor. Although this is not an impediment to using the probe, the operator needs to accurately calibrate pulses at all power levels in each experiment. Figure

1 shows dramatic enhancements in SNR for NOE difference experiments collected on a $\sim 250 \mu\text{M}$ sample of taxol compared to the sample spectra collected on a conventional system. The spectra collected with the HTS probe (top) contained numerous NOEs that were not observed using the conventional probe (bottom). These NOEs are consistent with the known structure of taxol.

High Field EPR of Fullerene Adducts Radical Anions

Maniero, A.L.,* NHMFL

Zoleo, A., Univ. of Padova, Italy, Physical Chemistry

Brustolon, M., Univ. of Padova, Italy, Physical Chemistry

The C_{60} high electronegativity makes it an excellent electron acceptor and, as a fulleride, it becomes a very attractive electron reservoir. A fundamental question underlying the application of C_{60} to problems of charge separation and storage is the extent to which the properties of C_{60} are retained when it is functionalized. Functionalization of the C_{60} aims to prepare compounds that present a higher solubility or an ability to bind to an inert matrix or, allowing their utilization in producing new materials.

An interesting class of fullerene derivatives is that of fulleropyrrolidines, prepared by 1,3-dipolar cyclo addition of azomethine ylides to C_{60} . Elucidation of the electronic structure of reduced fulleropyrrolidines becomes important as these compounds are extensively used as electron-accepting units in electro- and photo-active dyads.

We investigated radical monoanions of several fulleropyrrolidine mono- and bisadduct derivatives in MeTHF solution and glassy phase by cw and pulsed X-band EPR and cw HF-EPR spectroscopy. In this report we present the results obtained by HF-EPR at frequencies $\nu = 110$ and $\nu = 220$ GHz.

Fullerene bisadducts CIS1 and CIS3 (see Figure 1), with an aliphatic chain connecting the two N-containing 5-member rings linked to the C_{60} molecule, show in liquid solution four lines with strongly temperature dependent intensity ratios. The signals are due to anion conformations (in dynamic equilibrium one with respect to the others) characterized by slightly different geometry and spin density distribution, producing very small difference in g values ($g_{\text{max}} = 1.3 \cdot 10^{-4}$ for CIS1 and $g_{\text{max}} = 6.5 \cdot 10^{-4}$ for Cis3). Rigid phase spectra recorded at 110 GHz (Figure 1) present unstructured lineshape with $B_{\text{pp}} = 15$ G for CIS1 and $B_{\text{pp}} = 30$ G for CIS3, probably due to the presence of the different conformers having different g tensor anisotropy along with g strain.

Very different behavior is shown by the more symmetric fullerene mono and bisadducts NTEG, TRANS1 and TRANS2 reported in Figure 2. In liquid solution a single line ($B_{\text{pp}} = 0.6 - 0.8$ G) is recorded due to the presence of only one stable anion conformation. Glassy phase HF-EPR spectra show powder lineshape with resolved g tensor components. In Figure

2 spectra at $\nu = 220$ GHz are reported as a function of the g value. The g tensor principal values have been determined by simulation of the powder spectra recorded using DPPH as internal standard. We have correlated the different g tensor symmetry (quasi-axial for TRANS1 and rhombic for NTEG) to the different symmetry of the respective spin density distribution (C_{2h} symmetry for TRANS1 and C_s symmetry for NTEG).

Spin density distributions have been calculated for an optimized (PM3 method) molecular geometry by UHF method using a semiempirical Hamiltonian.

Thanks to the enhanced resolution of the HF-EPR technique, for the first time the g tensor parameters of some fullerene adducts monoanions have been measured and different conformers characterized by very close g factors have been detected, which makes possible a better understanding of the electronic properties of these systems.

* Present address: Dept. of Physical Chemistry, University of Padova, Italy

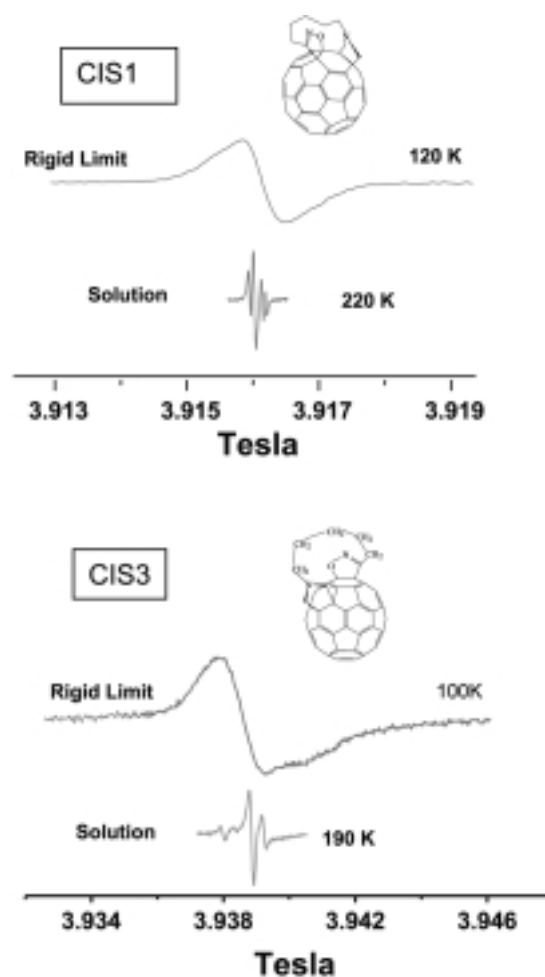


Figure 1. HF-EPR spectra recorded at $\nu = 110$ GHz in MeTHF liquid solution and glassy phase of CIS1 and CIS3 fullerene bisadduct monoanions.

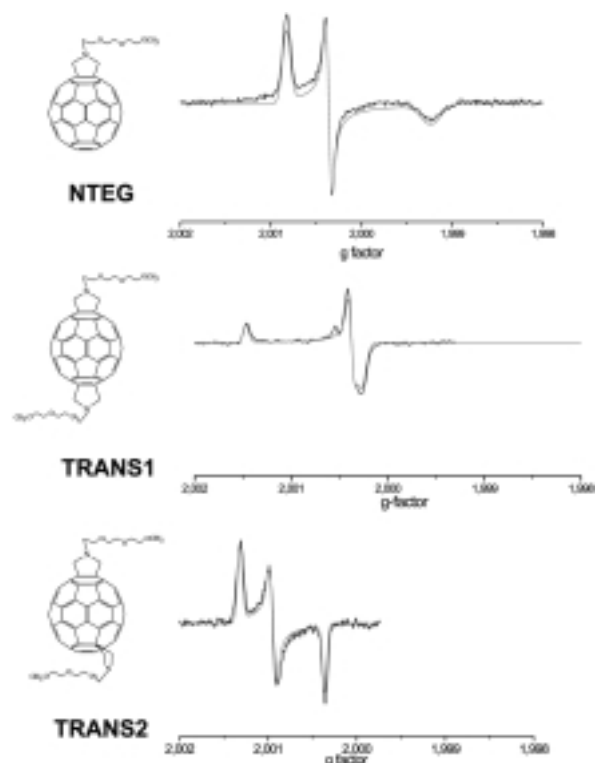


Figure 2. HF-EPR spectra and simulations at $\nu = 220$ GHz in MeTHF glassy phase of NTEG, TRANS1 and TRANS2 fullerene adduct monoanions. Spectra are shown as a function of the g factor.

High Field EPR Study of Salts of TDAE with Fullerene Derivatives

Maniero, A.L.,* NHMFL

Pasimeni, L., Univ. of Padova, Italy, Physical Chemistry

Brunel, L.-C., NHMFL

In the organic charge-transfer complex TDAE- C_{60} the role of the donor molecule is not ascertained so far. Several models were proposed to explain ferromagnetism at low temperature starting from the assumption that the spin ordering occurs mainly in the C_{60}^- anions, while the TDAE $^+$ cations, also containing an unpaired electron, are usually neglected. In fact, although for TDAE $^+$ - C_{60}^- we expect to observe two singlet lines, one corresponding to each molecular species, EPR measurements at X-band show the presence of only one line, which is usually assigned to the C_{60}^- .

To shine more light on this point we need a more sensitive spectroscopic tool capable to disclose small anisotropies in the g tensors of the involved paramagnetic species. An increase in the spectral resolution of inhomogeneously broadened EPR lines can be achieved by detecting EPR signals at high magnetic fields.

We investigated, by HF-EPR salts, of TDAE with a series of fullerene derivatives. EPR spectra contain two lines due to

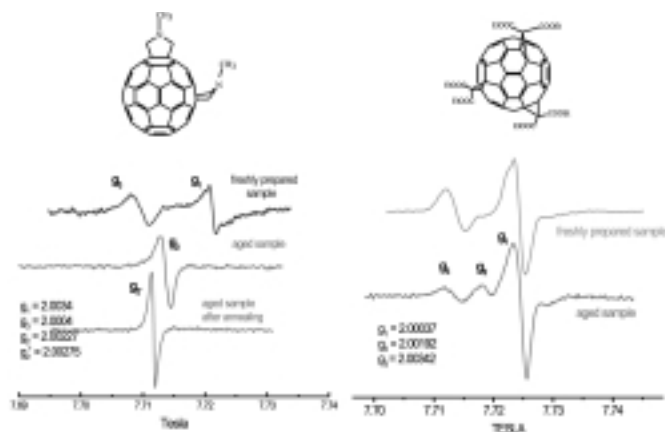


Figure 1. HF-EPR spectra recorded at $\nu = 220$ GHz and $T = 5$ K of two TDAE / fullerene derivatives salts. Fullerene derivative molecular structures are shown in the figure.

separated TDAE $^+$ ($g = 2.0034$) and fullerene $^-$ ($g = 2.0004$) radical ions. An additional line appears at intermediate g value that is attributed to the interacting radical ion pair. The relative intensity of the lines was found to depend on sample preparation and it changes also with time (Figure 1). Resonant frequencies remain almost unaltered by varying the temperature over a wide range (300 to 5 K).

An exception to this behavior is given by the salt of TDAE with N-Methylfulleropyrrolidine (NMeC $_{60}$) whose HF-EPR spectra exhibit features similar to those observed for TDAE- C_{60} ¹. The spectrum shows a marked g factor anisotropy with a selective

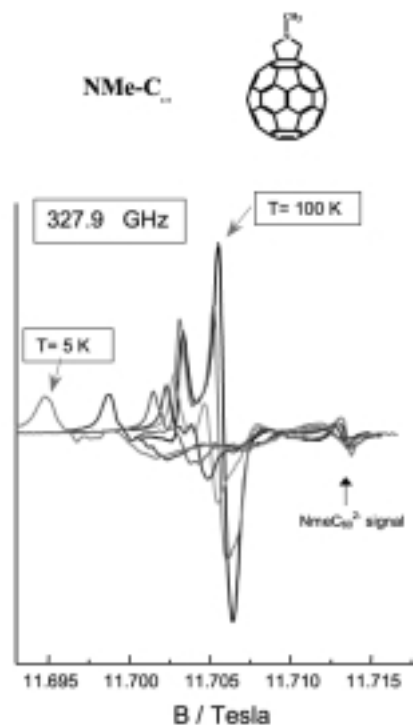


Figure 2. HF-EPR spectra of the TDAE/NMeC $_{60}$ salt recorded at $\nu = 328$ GHz as a function of the temperature. Resonant fields are downshifted when the temperature decreases. The signal at higher fields is attributed to NMeC $_{60}$ dianion.

downshift of the resonant fields more pronounced in the lower part of the spectrum profile below 80 K (Figure 2). The results are explained by one-dimensional short-range order effects between spins with inequivalent g tensors due to TDAE⁺ and N-Methylfulleropyrrolidine⁻ centers.

HF-EPR spectra provide evidence that in, TDAE/Fullerene derivatives salts, cation, and anion give rise to interacting species both participating to magnetic susceptibility.

¹ Maniero, A.L., *et al.*, Solid State Commun., **106**, 727 (1998).

* Present address: Department of Physical Chemistry, University of Padova, Italy

High Frequency EPR Spectra of Nitroxides in Single Crystal: The Role of “Forbidden” Transitions

Maniero, A.L.,* NHMFL

Brunel, L.-C., NHMFL

Brustolon, M., Univ. of Padova, Italy, Physical Chemistry

Segre, U., Univ. of Modena, Italy, Chemistry

Nitroxide spin probes are widely used to test the structure and dynamics of several materials and biological systems. The availability of high magnetic field allows recording high frequency EPR spectra (HF-EPR) with better resolution and obtaining more detailed information than traditional X band EPR. Analysis of HF-EPR spectra requires that the role of the different magnetic interactions in determining the spectral features is fully considered and that the usual approximations made in analyzing X band spectra are critically revised.

The spin Hamiltonian for an unpaired electron spin coupled to an $I = 1$ nuclear spin and interacting with an external magnetic field B_0 given by:

$$H = H_e + H_n + H_q + H_c = \mu_B B_0 \cdot g \cdot S - \mu_N g_N B_0 \cdot I + I \cdot Q \cdot I + S \cdot A \cdot I \quad (1)$$

Because of the relative strength of the two Zeeman terms H_e and H_n , the electron magnetic moment is quantized along the external magnetic field direction, while the nuclear magnetic moment is quantized along the resultant of the external and hyperfine fields. In the case of X band ($\nu \sim 10$ GHz) EPR spectra of nitroxide radicals the effect of H_n can be neglected with respect to H_e and the allowed transitions are obtained by the usual “selection rule” $\Delta M_S = 1$, $\Delta M_I = 0$.

We have performed full diagonalization of the spin Hamiltonian¹ for different microwave frequency ranges and we have found that when $\nu > 100$ GHz “forbidden” transitions ($\Delta M_I \neq 0$) contributes as well to the absorption spectrum. In Figure 1 positions and intensities of the EPR transitions are reported as a function of the angle between the magnetic field direction and the tensors symmetry axis for different microwave frequencies.

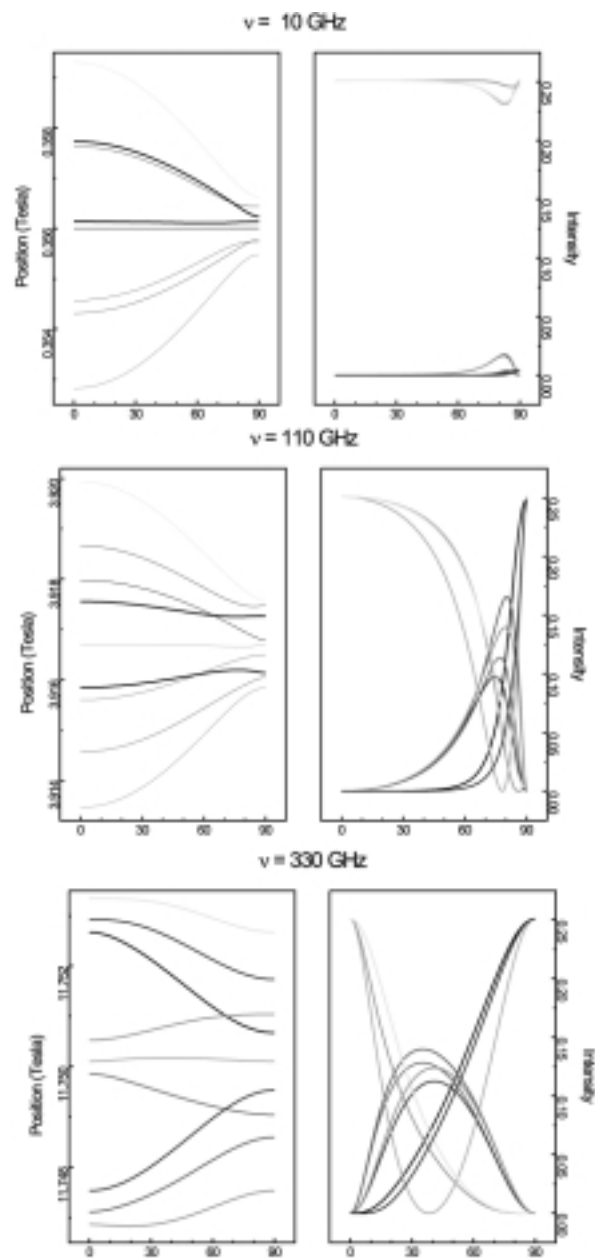


Figure 1. Positions and intensities of the EPR transitions as a function of the angle between the magnetic field direction and the symmetry axis of the magnetic tensors. (Parameters: $g = 2.0064$, $A_{\parallel} = 91$ MHz, $A_{\perp} = 16$ MHz, $Q_{\parallel} = -2$ MHz, $Q_{\perp} = 1$ MHz).

Single crystals of tempone nitroxide diluted in tetramethyl-1,3-cyclobutanedione have been obtained¹ and HF-EPR spectra at frequencies in the range 110 to 380 GHz have been recorded at different orientations of the magnetic field. Comparison with theoretical simulations allows accurate determination of the magnetic interaction tensors. In Figure 2 some HF-EPR spectra at different microwave frequencies and magnetic field orientations are reported along with simulations obtained by full diagonalization of the spin Hamiltonian.

¹ Bonon, A., *et al.*, Phys. Chem. Chem. Phys., **1**, 4015 (1999).

* Present address: University of Padova, Italy

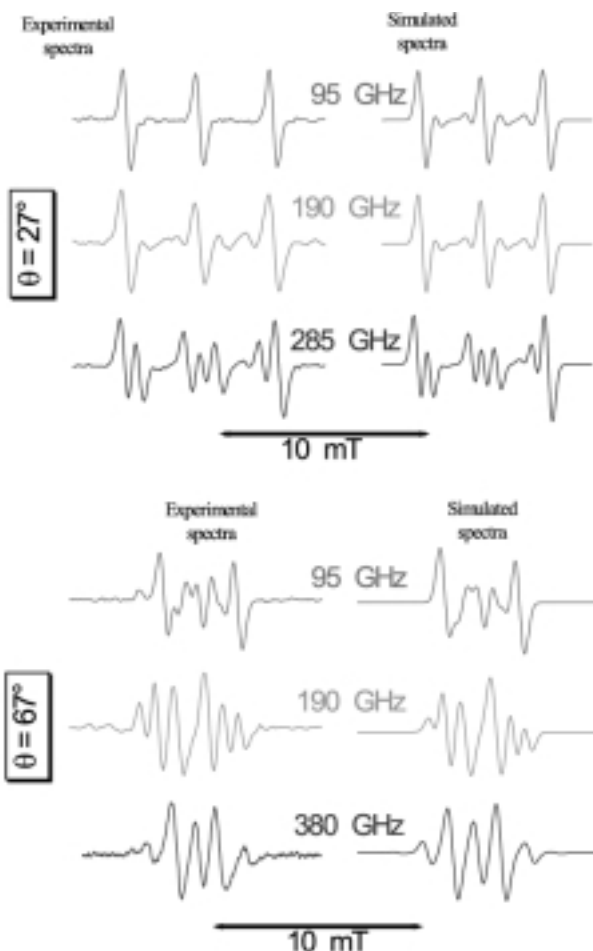


Figure 2. Experimental and simulated spectra of tempone nitroxide in a single crystal. HF-EPR spectra at different microwave frequencies are shown for two different magnetic field orientations (θ is the angle between the magnetic field and the A_{ZZ} directions). Centers of the spectra are shifted to allow their comparison. Principal values of the interaction tensors: $g = (2.0094, 2.0060, 2.0026)$, $Q = (1.15, 0.50, -1.65)$ MHz, $A = (16.27, 15.49, 91.06)$ MHz.

Solid State NMR Study of Highly Coupled Quadrupolar Nuclei at Very High Magnetic Field

Massiot, D., CRMHT-CNRS, Orléans, France

Quadrupolar nuclei ($I > 1/2$) in solid state compounds or material may undergo strong to severe broadening in solid state NMR experiments due to the “second order” quadrupolar interaction terms. Most of these quadrupolar nuclei are of major interest to solid state chemistry and material sciences (^{17}O , ^{23}Na , ^{27}Al , ^{71}Ga ...). The “second order” quadrupolar broadening that limits the resolution for spectra of powdered samples, is proportional to the inverse of the principal magnetic field and can thus be reduced in experiments carried out at very high magnetic fields. The expected gain is thus proportional to the square of the principal field both in resolution and sensitivity when quadrupolar interaction dominates the spectral response.¹

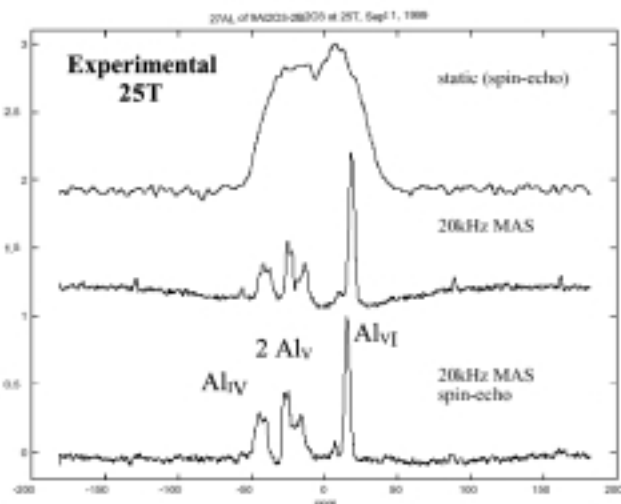


Figure 1. Experimental ^{27}Al MAS spectra of A_9B_2 at 25 T in static and 20 kHz MAS condition.

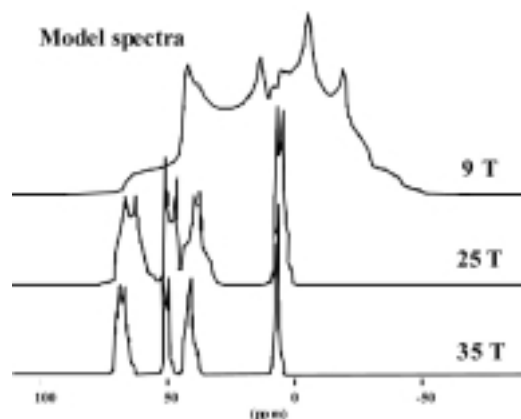


Figure 2. Model ^{27}Al MAS spectra of A_9B_2 for principal fields up to 35 T.

The ^{27}Al NMR spectra of the powder compound A_9B_2 ($9\text{Al}_2\text{O}_3 \cdot 2\text{B}_2\text{O}_3$), presented in Figure 1 have been obtained using the 25 T Keck magnet and give a convincing example of the increased resolution obtained at very high field for a second order broadened quadrupolar spectrum. At this high magnetic field, associated with fast magic angle spinning, the four aluminum sites (Al_{IV} , 2Al_{V} , and Al_{VI}) are almost separated, and their chemical shifts and relative abundance can be measured accurately in a simple one dimensional experiment. At lower fields these different sites completely overlap and could only be separated using two dimensional experiments like Dynamic Angle Spinning (DAS) or Multiple Quantum MAS (MQ-MAS), at the cost of experimental time and simplicity of the interpretation. Other experiments have been carried out on ^{71}Ga NMR, also providing clear illustration of the obtained increased resolution. From these results it is possible to extrapolate to the even higher fields of 35 T, which would increase the resolution and open the way to better characterization of the local environment of these quadrupolar nuclei in crystalline compounds and amorphous materials (see Figure 2).

¹ Massiot, D. *et al.*, C.R. Acad. Science Paris (1998).

Structural Features of the Eukaryotic U2snRNA-Intron Branch Site Pairing

Newby, M.I., NHMFL/FSU, Institute of Molecular Biophysics

Greenbaum, N.L., NHMFL/FSU, Institute of Molecular Biophysics, and Chemistry

The removal of noncoding sequences (introns) from eukaryotic precursor mRNA occurs via specific RNA-RNA and RNA-protein interactions in the spliceosome. One such interaction involves basepairing of the U2 small nuclear (sn) RNA with a conserved branch site sequence of the intron, resulting in the bulging of an adenosine that is critical in splicing. Chemical mapping studies of *S. Cerevisiae* and several other species identify a pseudouridine base in the U2snRNA (Figure 1) opposing the branch site. The discovery of this particular modified base implies that it is conserved and necessary for correct branch site structure formation *in vivo*.

The goal of this project is to determine the structure of the U2snRNA-intron branch site interaction by solution NMR spectroscopy. Oligonucleotide fragments representing the paired region with and without a pseudouridine (Figure 2) were chemically synthesized and deprotected according to standard phosphoramidite chemistry to assess the structural role of the modified base at the branch site. Base-ribose connectivities made from NOESY spectra of non-exchangeable protons are indicative of a predominantly A-form helical structure in both samples. Basepairing in the constructs was verified by imino proton resonances observed in NOESY spectra of exchangeable protons, and helical regions of both constructs exhibited similar imino-imino and imino-amino NOEs. Adenosine H2 NOEs in the unmodified constructs are typical of standard A-form geometry, however, the lack of NOEs to the branch site adenosine H2 proton in the modified molecule is clear evidence of an extrahelical adenosine conformation. Longitudinal (T_1) relaxation times were measured for the modified and unmodified constructs to examine global correlation times and to assess local motions on the NMR timescale for bulge-region base protons. T_1 was measured by inversion-recovery experiments, where $T_1 = \tau_{\text{null}}/\ln 2$. The unmodified molecule exhibits comparable T_1 relaxation times for all adenosine H2 protons observed. In the modified construct, however, the adenosine immediately adjacent to the branch site adenosine exhibits a T_1 relaxation time that is approximately 40% faster than those of helical adenosine H2 protons, suggesting that the cross-strand U2snRNA pseudouridine stabilizes the bases adjacent to the branch site adenosine. Ribose $J_{\text{H1}'\text{-H2}'}$ couplings observed by DQF-COSY spectra for pseudouridine-modified and unmodified sequences indicate that the modified construct has C2'-endo sugar pucker character for residues in the bulge region, whereas equivalent spectra show normal C3'-endo ribose conformations for corresponding sugars in the unmodified construct. These data indicate that backbone geometry in the bulged region of the molecule is different in the presence of the pseudouridine.

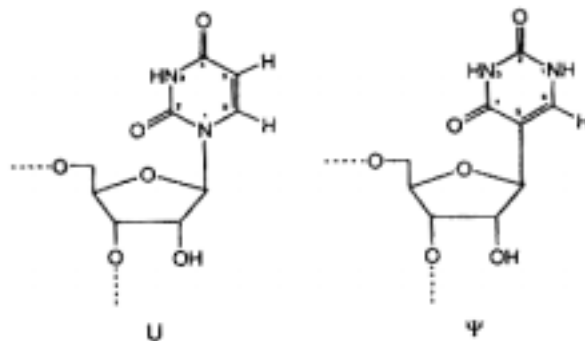


Figure 1. A pseudouridine has greater hydrogen bonding capability than a uridine.

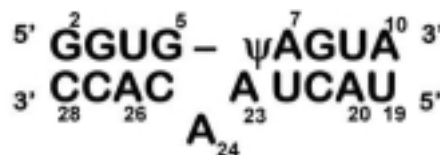


Figure 2. U2snRNA-intron pseudouridine-modified (Ψ) duplex construct. The unmodified duplex contains a uridine in place of the pseudouridine.

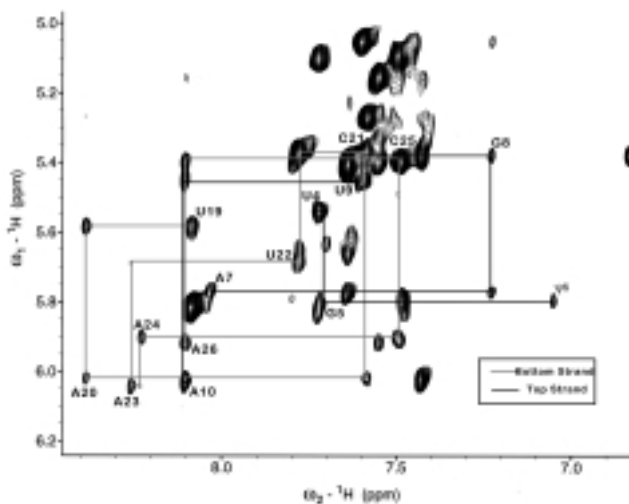


Figure 3. Aromatic-anomeric region of a NOESY spectrum of non-exchangeable protons in a pseudouridine-modified U2snRNA-intron construct. Lines indicate base-H1' sequential walk for both strands of the duplex shown in Figure 2. The sample is ~1 mM RNA in 10 mM sodium phosphate, 50 mM sodium chloride, and 0.1 mM EDTA in D₂O, pH~6.3. The spectrum was acquired at 20 °C on the 720 MHz Varian Unity Plus spectrometer at the NHMFL, with a mixing time of 350 msec.

Multifrequency EPR Spectra of Molecular Oxygen in Solid Air

Pardi, L. A., IFAM – CNR, Pisa, Italy

Krzystek, J., NHMFL

Telser, J., Roosevelt Univ., Chemistry

Brunel, L.-C., NHMFL

O₂ is a paramagnetic molecule with a $^3\Sigma_g^-$ ground state. In the gas phase, its EPR spectrum is fairly complicated due to the coupling of orbital angular momentum L , spin angular momentum S , and the nuclear angular momentum N . The spectrum shows a fine structure in which the dipolar and spin-orbit components play the major role.

In condensed phase the rotations and vibrations of the molecules are efficiently quenched and the spectrum is expected to be that of a simple spin triplet as suggested by magnetic measurements on solid and liquid oxygen. Due to the large zero field splitting (zfs) this triplet molecule is expected to be EPR-silent at low frequencies. With the development of high frequency and high field EPR spectroscopy (HF-EPR), molecular oxygen became observable mainly as an undesired impurity in low temperature experiments, but no systematic study of the spectrum has been undertaken. In Figure 1 we show the transition energy dependence of the observed resonances in a solid air sample at 5 K and in the 0 to 550 GHz frequency range (0 to 18 cm⁻¹). The spectra were satisfactorily interpreted within a spin triplet mode with zfs parameters $D = +3.6$ cm⁻¹ and $E = 0$, and $g(\text{isotropic}) = 2.00$ as shown by the simulated curves. This D value in the solid correlates nicely with that reported for the molecule in the gas phase.

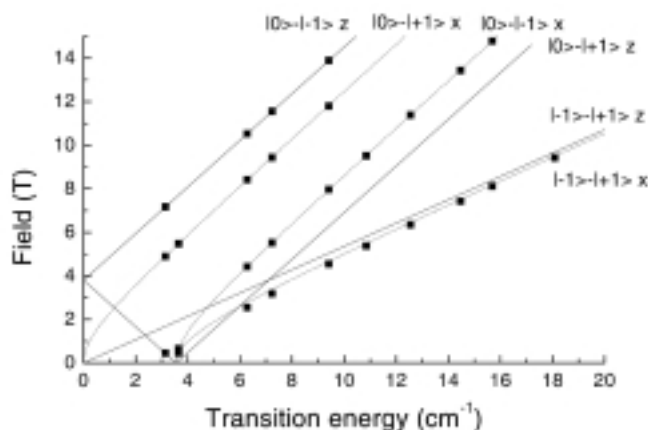


Figure 1. Magnetic resonance field vs. transition energy dependence for solid oxygen in frozen air at 5 K. The squares represent experimental points while the curves were calculated using the spin Hamiltonian parameters as in the text. The particular transitions are identified and labelled accordingly.

Jet Fuel Chemical Composition, Weathering, and Identification as a Contaminant at a Remediation Site, Determined by Fourier Transform Ion Cyclotron Resonance Mass Spectrometry

Rodgers, R.P., FSU, Chemistry

Blumer, E.N., FSU, Chemistry

Freitas, M.A., NHMFL

Marshall, A.G., NHMFL/FSU, Chemistry

We have characterized a jet fuel (JP-8) contaminated site and compared its chemical constituents to a set of unweathered JP-4, JP-5 and JP-8 weathered standards by use of an all-glass heated inlet system (AGHIS) coupled to a homebuilt 6.0 T Fourier transform ion cyclotron resonance (FT-ICR) mass spectrometer. From as little as a 1 μ L septum injection of JP-8, JP-5, or JP-4 into the AGHIS (see figure), we obtained high-resolution mass spectra containing ~ 400 peaks, 50 m/z 280, with as many as 4 peaks at the same nominal mass. A molecular formula (elemental composition) could be assigned to each peak, based solely on accurate mass measurement to ± 0.8 ppm. With increased “weathering” (i.e., evaporation), JP-8 exhibited significantly increased number and relative abundance of higher-mass ($200 < m/z < 250$) species, in accord with previously observed increase in gas retention times with increased weathering. By extraction and subsequent FT-ICR mass analysis of JP-8 contaminated soil, we were able to identify and correlate many species to those present in the unweathered/weathered standards, as well as identify a small number of new species attributed to degradation products from prolonged weathering and matrix components arising from species extracted from the soil.

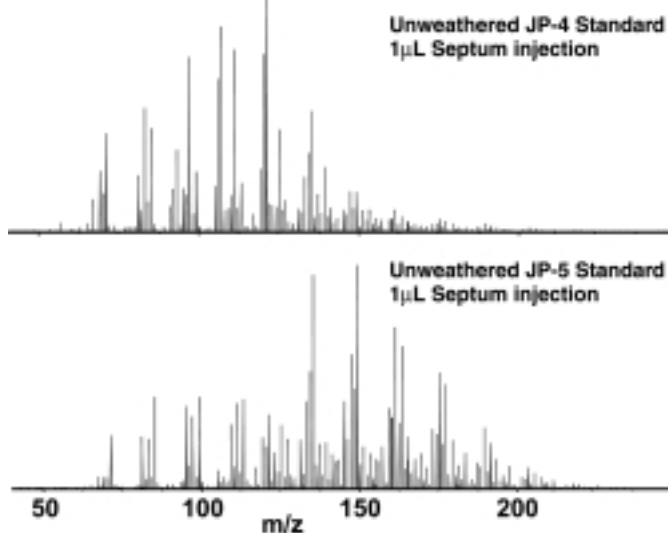


Figure 1. FT-ICR spectra of 1 μ L of jet fuel injected into an all glass heated inlet system. Upper panel: JP-4. Lower panel: JP-5.

Acknowledgements: The authors thank Daniel McIntosh for machining all of the custom parts required for the 6 T instrument construction and Randall Pelt for the glasswork on the AGHIS. The authors also thank Christopher L. Hendrickson and John P. Quinn for many helpful discussions. This work was supported by the NSF National High-Field FT-ICR Mass Spectrometry Facility (CHE-94-13008), Florida State University, and the NHMFL at Tallahassee, Florida.

¹ Rodgers, R.P., *et al.*, *Anal. Chem.*, **71**, 5171-5176 (1999).

High Field Solid-State NMR of Titanium/Silica Low-Thermal-Expansion Glass and Titania Silicalite Catalysts

Stiegman, A.E., FSU, Chemistry

We are interested in investigating the properties of binary titania-silica oxide materials. Several specific classes of these materials are of interest due to their useful properties. In particular, amorphous titania/silica glasses are of interest because of their unusually low coefficient of thermal expansion (CTE) while titanium silicalite (TS-1) zeolitic materials are active as selective oxidation catalysts. Since these useful properties arise from the properties of the titanium as it occurs in the silica matrix, there has been a considerable amount of work done to elucidate its structure. This has been a difficult task since these materials tend to be weak Raman scatterers in all but the highest Ti concentrations. X-ray absorption (EXAFS and XANES) studies of these systems have indicated that the titanium is 4-coordinate and not 6-coordinate, which has led to a general view that the titanium simply substitutes for silicon in the tetrahedral sites of the silicon. While this may prove to be true, data supporting this structure over other four-coordinate structures of lower symmetry is not compelling. Direct observation of the titanium through NMR techniques would provide a great deal of insight into this problem. Unfortunately, titanium is a very poor NMR nucleus. Its two active nuclei (⁴⁷Ti and ⁴⁹Ti) have low natural abundances, large nuclear quadrupoles, and small magnetogyric ratios. This leads to low sensitivity and broad resonances. Most observations of Ti through NMR are limited to high symmetry materials such as the binary oxides (anatase and rutile) and high symmetry perovskites such as barium titanate. To date, attempts to observe Ti in catalytic materials (TS-1) and in low thermal expansion glasses have not been successful.

Recently, collaborative work between our group at the Chemistry Department at Florida State University and at the NHMFL has been focussed on observing the Ti nucleus in these types of materials. This has been undertaken to ascertain whether high magnetic fields in conjunction with new multinuclear probes can measure spectra of this difficult nucleus. Preliminary studies of bulk oxides have been extremely promising in demonstrating the value of high field NMR. We were able to obtain high quality solid-state NMR spectra of the titanium nucleus by application of high magnetic field (833 MHz). Figure 1 shows static powder spectra for the bulk TiO₂ oxides of the (a) anatase

and (b) rutile phase. Comparison of these to published spectra collected on a lower field instrument (500 MHz) indicated the dramatic improvement in sensitivity and resolution that can be realized at high fields. Currently, studies of titanium in low CTE glass and titanium silicalite are underway, and we are confident that insights into this important material will be realized.

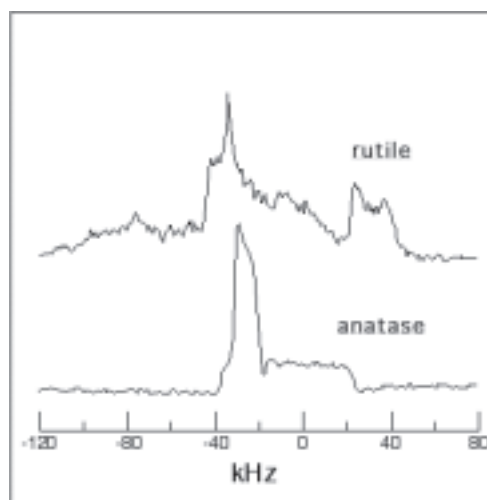


Figure 1. Static powder spectra for the bulk TiO₂ oxides of the (a) anatase and (b) rutile phase.

EPR from “EPR-Silent” Species: High Frequency and High Field EPR Spectroscopy of a Vanadium(III) Molecular Complex

Telser, J., Roosevelt Univ., Chemistry

Krzystek, J., NHMFL

Van Tol, J., NHMFL

The recently developed technique of high frequency, high field EPR (HF-EPR); $\nu > 90$ GHz; B up to 25 T) has proven to be effective at elucidating the electronic structure of integer-spin systems.¹⁻⁴ Of particular value is the combination of the multi-frequency capability of the EPR spectrometer employed here with the ability to perform continuous field sweeps over a broad range (0 to 25 T). This allows one to choose a convenient parameter “window” to observe most, if not all, of the multitude of transitions characterizing a high-spin, non-Kramers spin species.

We report here the use of HF-EPR to investigate an “EPR-silent” non-Kramers system, V³⁺ ($3d^2$, $S = 1$), in the complex V(acac)₃, where acac is the chelating ligand, 2,4-pentanedionate.⁵ This system is of specific interest as a relatively rare example of a stable vanadium(III) complex, but given that $3d^2$, $S = 1$ complexes are relatively uncommon, it is of general interest as well. Furthermore, our efforts thus far on “EPR-silent” integer-spin systems have emphasized those with $S = 2$,^{1,3,4} which can often be EPR-visible using conventional spectrometers, when the molecular symmetry is rhombic ($x \ y \ z$), as opposed

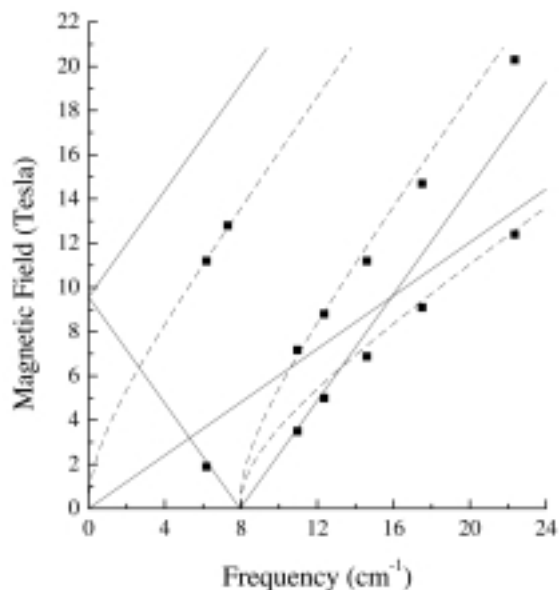


Figure 1. Resonant EPR magnetic field versus energy for $V(acac)_3$ as a solid pellet. Squares represent experimental points, and the lines represent theoretical curves for the canonical transitions with the magnetic field along z (parallel, solid lines) and along x (perpendicular, dashed lines). The simulation parameters for both the powder pattern and resonant field plots are: $D = +7.95 \text{ cm}^{-1}$, $E = 0.0$, isotropic $g = 1.78$.

to axial ($x = y = z$). Systems with $S = 1$, however, are EPR-silent unless the molecular symmetry is close to cubic ($x = y = z$). Thus, the application of HF-EPR to $S = 1$ systems is important in demonstrating the breadth of applicability of the HF-EPR technique. From an experimental point of view, this study also shows the applicability of the high-homogeneity resistive “Keck” magnet in recording spectra at these very high fields.

Figure 1 presents experimental and theoretical resonant HF-EPR transitions for solid $V(acac)_3$. The theoretical lines have been calculated by full-matrix solutions to the spin Hamiltonian for an $S = 2$ system. The resulting Hamiltonian parameters are: $D = +7.95(5) \text{ cm}^{-1}$, $E = 0.0(1)$, and $g_{\parallel} = g_{\perp} = 1.78(2)$. These results are in agreement with a magnetic susceptibility study of this compound,⁵ however the present study shows that the molecule has no rhombic distortion ($E = 0$), which is consistent with its absence in the solid state structure.⁶ Note that magnetic measurements are rather insensitive to the E parameter. The data at very high field ($< 25 \text{ T}$) were critical in the analysis, and further suggest that second-order electronic Zeeman terms may be relevant to explaining behavior at very high-fields. HF-EPR data is combined with earlier electronic absorption data to provide a complete picture of the electronic structure of V^{3+} in this chemical environment. This analysis requires treatment of the complete $3d^2$ electronic configuration, including singlet excited states.

¹ Goldberg, D.P., *et al.*, *J. Am. Chem. Soc.*, **119**, 8722 (1997).

² Barra, A.-L., *et al.*, *Angew. Chem. Intl. Ed. Engl.*, **36**, 2329 (1997).

³ Telser, J., *et al.*, *Inorg. Chem.*, **37**, 5769 (1998).

⁴ Krzystek, J., *et al.*, *Inorg. Chem.*, **38**, 6121 (1999).

⁵ Gregson, A.K. *et al.*, *Inorg. Chem.*, **17**, 1216 (1978).

⁶ Morosin, B. and Montgomery, H., *Acta Cryst.*, **B25**, 1354 (1969).

Developing Nano-Liter Probes for High Resolution Biomolecular NMR in Ultra High Field NMR Magnets with Low Homogeneity **IIHRP**

Webb, A., Univ. of Illinois, Electrical Engineering

Subramanian, R., Univ. of Illinois, Electrical Engineering

Gor'kov, L., NHMFL

Brey, W., NHMFL

Logan, T.M., FSU, Chemistry/NHMFL

Sensitivity is the Achilles' heel of NMR spectroscopy. One approach to improving sensitivity is to use higher field NMR magnets. It is more economical, however, to produce a field of lower homogeneity than the 1 part per billion commonly obtained in commercial high resolution NMR magnets. To circumvent this low homogeneity, it is possible to shrink the sample size to where the homogeneity is high enough for high resolution NMR, and, when shrinking the sample size, it is preferred to generate solenoidal coils to optimize the filling factor. The design and use of microcoil probes having 5 nL to 1 μL detection cells offer substantially greater mass sensitivity compared to conventional NMR probes have been demonstrated for small molecule NMR. In this project, we are extending this microcoil technology to develop NMR microcoils suitable for high resolution biomolecular NMR spectroscopy of proteins, with the ultimate aim of the project being to build a triple resonance microcoil probe with pulsed field gradient capability to perform biological NMR experiments on the 833 MHz NMR spectrometer. Several challenges have to be overcome in order to accomplish this goal.

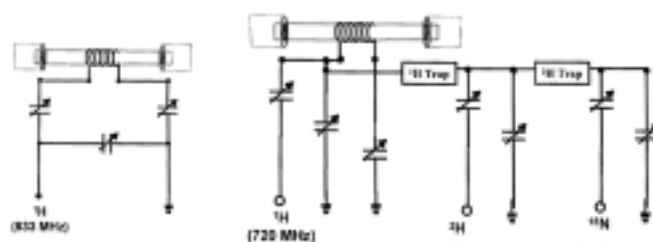


Figure 1. Schematic wiring diagram showing the electrical circuits used for the 833 MHz microcoil (left) and the 720 MHz double-resonance (proton and nitrogen) microcoil.

The design for triple resonance coils having fixed frequencies of ^1H , ^{13}C , and ^{15}N has been completed. The three channels are impedance matched to 720, 110.5, and 72.9 MHz, corresponding for use on the 720 MHz instrument at the NHMFL. The dimensions of the probe fit a standard narrow bore magnet (of 51 mm inner diameter), with an observe volume of 13.5 microliters. The three channels are generated on the same solenoidal coil, which also acts as a receive coil using a circuit similar to that shown below. Z-axis pulsed field gradients have been designed and are currently being built.

To extend this technology to highest available superconducting fields, a 10 microliter observe volume probe has been built with the (^1H -only) coil tuned to 833 MHz. In addition, the probe has an external lock capability. Tuning is accomplished by the circuit shown in Figure 1. Installation and testing of these probes is scheduled to begin early 2000.

Peptide Binding by a Prokaryotic SH3-Like Domain from the Diphtheria Toxin Repressor Protein

Wylie, G.P., FSU, Chemistry

Mertz, L., FSU, Chemistry

Murphy, J.R., Boston Univ., Medicine

Logan, T.M., NHMFL/FSU, Chemistry

We have previously determined the solution structure of the C-terminal domain of the diphtheria toxin repressor (DtxR), and found that it is structurally homologous to eukaryotic SH3 domains. Furthermore, we demonstrated binding of a proline-containing peptide that corresponds to residues 125-139 of intact DtxR, by the C-terminal domain, providing the first indication that the structure and function of this protein-binding domain is more widely conserved than previously known. Significantly, the structure and function have been conserved, while the sequence has not. There is only $\sim 7\%$ sequence similarity between the DtxR and typical eukaryotic SH3 domains. Therefore, the chemistry of peptide recognition and binding by the DtxR SH3 domain must differ fundamentally from that of eukaryotic SH3 domains. The objective of this project is to characterize the binding affinity and to determine the structure of the DtxR SH3 domain complexed to this internal peptide.

Structural studies of the uncomplexed protein (residues 144-226) are underway. As expected, initial assignments indicate little structural change upon deleting 14 amino acids from the N-terminus, which were not structured in our previous study. Previous experiments indicated that one or more histidines may be involved in binding. To follow changes in histidine environment upon titration with peptide, we are collecting 1D TOCSY spectra on solvent-exchanged DtxR(144-226). The solvent exchange reduces the intensity of most amide resonances, and the un-exchanged amide resonances are reduced further by the spinlock, allowing us to clearly follow the C^δH and $\text{C}^\epsilon\text{H}$ resonances of the three histidines in the protein (Figure 1). By using 1D NMR, we can use rather dilute protein solutions of $\sim 50 \mu\text{M}$. Our model for binding assumes a 1:1 stoichiometry, as observed in eukaryotic SH3 domains, with a high micro-molar dissociation constant. Several titrations have indicated that this model does not fit our data, while a model incorporating some degree of cooperativity better approximates the data. This cooperativity may arise from (1) slow binding involving conformational changes of the peptide, which must adopt a poly-proline type-II helix if it binds as in eukaryotic SH3 domains, or (2) a structural rearrangement of the protein

upon binding. The latter situation is not supported by the NMR data, as there are essentially no changes in any of the C^αH resonances involved in β -sheet formation. At this time, we are performing several different experiments to further identify the appropriate model for binding. Nevertheless, the fact that this SH3 domain does not appear to bind proline-containing peptides in a manner similar to eukaryotic SH3 domains is intriguing.

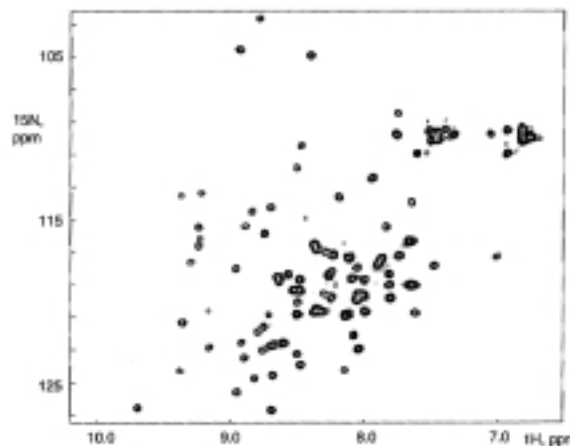


Figure 1. 2D spectrum of DtxR(144-226) indicating region of interest during the peptide titrations.

Acknowledgement: This work was supported by the American Heart Association.

Role of a 5' Methylguanosine Cap in the Structure of a Spliced Leader RNA

Yeager, S.J., NHMFL/FSU, Chemistry

Greenbaum, N.L., NHMFL/FSU, Chemistry, and Institute of Molecular Biophysics

Trans-splicing involves the transfer of a donor spliced leader (SL) RNA fragment to an acceptor precursor mRNA transcript. It is an essential process in the maturation of mRNA in certain organisms. The spliced leader has been proposed to operate as a translational enhancer signal during gene expression. *In vivo* this RNA fragment carries a trimethylguanosine (3MeG) nucleotide moiety covalently attached to the 5' terminus via a 5'-5' linkage (3MeG-5'pppSL). We hypothesize that the presence of the 5' cap effects the formation of a unique and stable structure of the SL. The goal of this research is to determine the solution structure of the 22-nucleotide spliced leader RNA fragment from the nematode *C.elegans* in order to understand the molecular basis of recognition by its receptor.

RNA samples were produced by *in vitro* transcription techniques with and without a 5' 7-methylguanosine cap (commercially available 7-methylguanosine was substituted for 3Me-guanosine in preliminary studies). A series of NMR experiments have

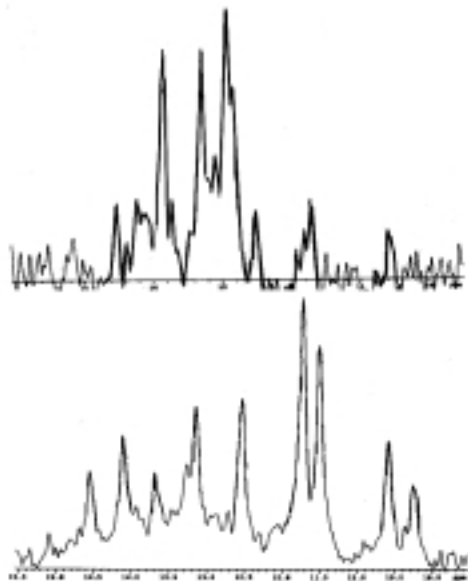


Figure 1. Imino proton regions of exchangeable ^1H spectra performed at 1°C . Top spectrum is capped RNA. Bottom spectrum is uncapped RNA.

been carried out on solutions containing approximately 1 mM RNA. Analysis of TOCSY spectra of aromatic protons of the uncapped molecule has verified that the folded SL adopts a single conformation. The pattern of imino proton resonances in spectra of exchangeable protons reveals both Watson-Crick and non-Watson-Crick base pairing and suggest a complex fold for the RNA. Imino proton resonances of the capped RNA were substantially altered in location and relative intensity. We conclude that the presence of a 5' cap induces a markedly different folded structure. In collaboration with Prof. Martin Schwartz's laboratory (Dept. of Chemistry, FSU), we have begun synthesis of a trimethylguanosine capped spliced leader that will be used for further structure determination.

GEOCHEMISTRY

Analysis of Organic Phosphorus in Surface Waters from the Florida Everglades by Capillary Electrophoresis and High Performance Liquid Chromatography Coupled to Inductively Coupled Plasma Mass Spectrometry

Bennett, L., NHMFL/FSU, Geological Sciences
 Salters, V.J.M., NHMFL/FSU, Geological Sciences
 Cooper, W., NHMFL/FSU, Geological Sciences

Nutrient loading has become a significant problem in many ecosystems, and especially in the Florida Everglades. Increases in phosphorus (P) have been linked to many alterations in this naturally oligotrophic ecosystem, including taxonomic shifts and eutrophication. A concerted effort to reduce phosphorus entering the Everglades was begun with the construction of the Everglades Nutrient Removal Project (ENR), the largest treatment wetland in North America. Verification of the efficacy of the ENR requires the development and application of specialized analytical techniques that can determine various organo-P species at environmentally significant levels.

Inductively coupled plasma mass spectrometry (ICP-MS) is a sensitive and selective technique for determining low levels (~ 1 ppb) of P in liquid matrices. Last year we demonstrated that ICP-MS analysis of Everglades water samples was superior to conventional colorimetric methods for total P analysis at both low P concentrations and at high organic carbon content.

This year we have coupled Capillary Electrophoresis (CE) and High Performance Liquid Chromatography (HPLC) with element-specific ICP-MS detection in order to quantitate individual types of organic phosphorus compounds in the Florida Everglades. Both are high resolution, physical separation methods that can isolate individual classes of organo-phosphates before P-specific detection. CE separates individual species in a microcolumn across which a high electric field is maintained. Separations are based on differences in charge and mass of the analytes. Owing to the complexity of natural water samples, many compounds have similar charge to mass ratios, and thus CE electropherograms obtained with non-specific detectors are broad distributions with little if any resolution of individual compounds. However, the separation of all compounds in a complex sample is not necessary when ICP-MS element-specific detection is employed, but rather only the separation of individual phosphorus species.

Interfacing a Capillary Electropherograph to the ICP-MS was accomplished by connecting the column to a micro-cross with a make-up flow and counter electrode which was inserted into a standard micro-flow nebulizer and spray chamber of the ICP source. An electropherogram of Everglades water is shown in Figure 1. The numerous discrete peaks in this electropherogram demonstrate the presence of several individual organo-phosphates.

HPLC is a column separation technique based on the distribution of solutes between mobile and stationary phases. The principal advantage of HPLC over CE is that fractions coming off the chromatography column can be collected and subjected to further analyses. When operated in the ion-pair mode (HPIPC), charged analytes can be separated in a pseudo ion-exchange manner. Again, by using the ICP-MS as a P-specific